Development 118, 705-717 (1993)
Printed in Great Britain © The Company of Biologists Limited 1993

W-sash affects positive and negative elements controlling c-*kit* expression: ectopic c-*kit* expression at sites of kit-ligand expression affects melanogenesis

Regina Duttlinger[1,2], Katia Manova[1,3,*], Tang Y. Chu[1], Corina Gyssler[1], Andrew D. Zelenetz[1], Rosemary F. Bachvarova[3] and Peter Besmer[1,†]

[1]Molecular Biology Program and [2]Graduate Program in Immunology, Sloan Kettering Institute and Cornell University, Graduate School of Medical Sciences, 1275 York Avenue, New York, NY 10021, USA
[3]Department of Cell Biology and Anatomy, Cornell University Medical College, 1300 York Avenue, New York, NY 10021, USA

*Permanent address: Institute of Cell Biology and Morphology, Bulgarian Academy of Sciences, Sofia, Bulgaria
†Author for correspondence

SUMMARY

The receptor tyrosine kinase c-*kit* and its cognate ligand KL are encoded at the *white spotting (W)* and *steel (Sl)* loci of the mouse, respectively. Mutations at both the *W* and the *Sl* locus cause deficiencies in gametogenesis, melanogenesis and hematopoiesis (erythrocytes and mast cells). The *W-sash* mutation differs from most *W* mutations in that it affects primarily mast cells and melanogenesis but not other cellular targets of *W* and *Sl* mutations. Thus, W^{sh}/W^{sh} mice are fertile and not anemic, but they lack mast cells in their skin and intestine and are devoid of coat pigment. Heterozygotes are black with a broad white sash/belt in the lumbar region. In order to determine the basis for the phenotypes of *W-sash* mice, we investigated c-*kit* RNA and protein expression patterns in adult W^{sh}/W^{sh} mice and during embryonic development. We show that c-kit expression is absent in bone-marrow-derived W^{sh}/W^{sh} mast cells, the fetal and the adult lung, and the digestive tract at embryonic day $13\frac{1}{2}$ ($E13\frac{1}{2}$), tissues that normally express c-*kit*. Unexpectedly, in $E10\frac{1}{2}$ and $11\frac{1}{2}$d W^{sh}/W^{sh} embryos, we found c-*kit* expression in the dermatome of the somites, the mesenchyme around the otic vesicle and the floorplate of the neural tube, structures known to express the c-*kit* ligand in wild-type embryos. The ectopic c-*kit* expression in W^{sh} homozygous embryos does not affect c-*kit* ligand expression. The presumed W^{sh}/W^{sh} melanoblasts appeared to be normal and, at $E10\frac{1}{2}$, similar numbers were found in normal and homozygous mutant embryos. At $E13\frac{1}{2}$ +/+ embryos had a graded distribution of melanoblasts from cranial to caudal with a minimum in the lumbar region. Whereas $E13\frac{1}{2}$ homozygous W^{sh}/W^{sh} embryos essentially lacked c-*kit*-positive cells in the skin, $E13\frac{1}{2}$ heterozygous W^{sh}/+ embryos had reduced numbers of melanoblasts compared to +/+ with few or none in the lumbar region (future *sash*). It is proposed that ectopic c-*kit* expression in the somitic dermatome affects early melanogensis in a dominant fashion. Molecular analysis of W^{sh} chromosomal DNA revealed a deletion or rearrangement in the vicinity of the c-*kit* gene. These results provide an explanation for the W^{sh} phenotype and have implications for the control of c-*kit* expression.

Key words: c-*kit* receptor, expression mutation, *W-sash*, negative and positive control elements, melanogenesis

INTRODUCTION

Mutations at the *white spotting (W)* and *steel (Sl)* loci in mice result in deficiencies in the production of three classes of cells: melanocytes, germ cells and hematopoietic cells (specifically erythrocytes and mast cells) (for reviews, see Russell, 1979; Silvers, 1979). The *W* and the *Sl* loci of mice, respectively, encode the proto-oncogene c-*kit*, a receptor tyrosine kinase of the PDGF receptor subfamily and the kit-ligand, KL, also designated steel factor (Besmer et al., 1986; Yarden et al., 1987; Majumder et al., 1988; Qiu at al., 1988; Chabot et al., 1988; Geissler et al., 1988; Nocka et al., 1989, 1990b,c; Zsebo et al., 1990a,b; Williams et al., 1990; Copeland et al., 1990).

Many independent mutations at the *W* locus have been described. The different alleles vary in their degree of severity in the heterozygous and the homozygous state, but most of them affect the different cellular targets of the mutations to comparable degrees (Silvers, 1979; Geissler et al., 1981; Lyon and Searle, 1989). The *W-sash* mutation

differs from most other *W* mutations in that only pigmentation and tissue mast cells are affected in homozygous mutant mice (Lyon and Glenister, 1982; Stevens and Loutit, 1982). Thus, homozygous W^{sh} mutant mice are fertile and not anemic, but they are black-eyed whites with small black patches around the ears and eyes and lack mast cells in their skin and intestine. Heterozygotes, from which the name is derived, have a broad white sash or band in the lumbar region.

The white sash of heterozygous W^{sh} mice differs from the pigmentation pattern of most mice with *W* mutations and reflects a dominant property of the mutation (Stephenson et al., 1985). Heterozygous *W* mutant mice with null mutations (*W* and W^{19H}) have a white belly spot of varying size, while heterozygous mutant animals with dominant *W* mutations are either black-eyed whites (W^{42}), or have a flecked appearance (W^{37}).

Melanocytes are derived from neural crest cells that migrate along a dorsolateral pathway away from the neural tube over the dermatomes of the somites (for a review see LeDouarin, 1982). They then spread through the dermis down to the ventral region of the body. Neural crest cell migration is first seen at rostral levels around E8½ and then proceeds in an anterior-to-posterior fashion (Rawles, 1947). By E11½ melanoblasts are found in the dorsal dermis in the trunk region (Rawles, 1947; Mayer, 1965; Serbedzija et al., 1990) and by E12½ the precursor cells have reached the ventral midline (Rawles, 1947). At E13½ some melanoblasts have moved from the dermis into the epidermis (Rawles, 1947; Mayer, 1973). The white skin of W^{v}/W^{v} mice as well as the white spots of *W*/+ and W^{v}/+ mice lack melanocytes (Silvers, 1956, 1979). The absence of melanocytes can be interpreted as a failure of the precursor cells to migrate, or as a failure to proliferate, or to survive. However, a defect in migration or failure to proliferate are not sufficient to explain the white belt in W^{sh}/+ mice.

During melanogenesis, c-*kit* function is necessary at around E14½, when melanocyte precursors migrate from the dermis into the epidermis (Mayers, 1973; Nishikawa et al., 1991). An earlier function for c-*kit* is suggested by the finding of synchronous c-*kit* and KL expression in melanoblasts found dorsally and laterally of the somites and in the somitic dermatome, respectively, at around embryonic day 10½ (Manova and Bachvarova, 1991; Matsui et al., 1990).

The molecular basis of the W^{sh} mutation is not known. In mutant mice in which all three targets are affected similarly, an intrinsic defect of c-*kit* receptor function is the probable cause of the mutation. Molecular analysis of several *W* alleles revealed missense mutations in c-*kit* which affect the c-*kit* kinase (Nocka et al., 1989, 1990a; Tan et al., 1990; Reith et al., 1990; for a review see, Besmer, 1991). The non-parallel display of mutant characteristics in W^{sh} mice might indicate that the mutation affects c-*kit* function in some cell types and not in others, possibly as a result of differential effects on c-*kit* transcription or post-transcriptional processing.

In an attempt to determine the basis of the phenotype of W^{sh} mice, we investigated c-*kit* expression in various tissues and cell types of homozygous mutant mice at various stages of development. We show here that some tissues and cell types that normally express c-*kit* lack expression in W^{sh}/W^{sh} mice. Interestingly, inappropriate c-*kit* expression was found in some tissues known to express the kit-ligand in normal mice during embryonic development. Analysis of chromosomal DNA from W^{sh}/W^{sh} mice by conventional and pulsed-field gel electrophoresis (PFGE) DNA blots indicated no alterations of c-*kit* exon and intron sequences but a deletion or rearrangement in the vicinity of the c-*kit* gene. Our results provide possible explanations for the pigmentation pattern of heterozygous and homozygous W^{sh} mice and define time points of c-*kit* function during melanogenesis. Also, our results have implications for transcriptional control of the c-*kit* proto-oncogene.

MATERIALS AND METHODS

Mice and embryos

C57BL/6J and C3H/HeJ mice were purchased from the Jackson Laboratory. C57BL/6 W^{sh}/W^{sh} mice were kindly provided by Dr Rudolf Jaenisch, MIT and 101 mice were provided by Dr L. B. Russell, Oak Ridge National Laboratories. Embryos were derived from appropriate matings of C57BL/6 W^{sh}/W^{sh} and C57BL/6J. The morning of vaginal plug was considered as day 0.5 p.c.

Mast cell cultures

Mast cells were grown from bone marrow of adult mice in RPMI-1640 supplemented with 10% fetal calf serum, 6% conditioned medium from WEHI-3B cells, non-essential amino acids, sodium pyruvate and 2-mercaptoethanol (5×10^{-5} M). Non-adherent cells were harvested and fed weekly and maintained at a cell density of 5×10^{5} cells/ml.

RNA and DNA isolation and blot analysis

Mast cells and mouse tissues were homogenized in guanidinium isothiocyanate and RNA isolated according to the method of Chirgwin et al. (1979). Total cellular RNA (mast cells: 1 μg, 2 μg and 5 μg; lung, brain and testis: 15 μg) was fractionated in 1% agarose-formaldehyde gels, transferred to nylon membranes (Nytran, Schleicher and Schuell) and prehybridization and hybridization performed as previously described (Lehrach et al., 1977; Nocka et al., 1989). The murine 1.4 kb c-*kit* cDNA labeled with ^{32}P-dCTP, prepared by the random primer method, was used as a probe for hybridization (Feinberg and Vogelstein, 1983).

DNA was extracted by standard techniques (Sambrook et al., 1989) and digested with restriction endonucleases (Boehringer Mannheim) in restriction buffer provided by the manufacturer. The DNA was fractionated in 0.8% agarose gels. The DNA was depurinated with 0.25 M hydrochloric acid for 5 minutes, denatured with 0.5 N sodium hydroxide for 5 minutes, neutralized with 1 M Tris, pH 5.0, 2 M sodium chloride for 5 minutes and vacuum-transferred (LKB, Pharmacia) to nylon membranes (Zetabind; AMF Cuno, Meridian, CT) in 1× SSC (0.15 M sodium chloride, 0.015 M sodium citrate) for 3 hours. DNA was crosslinked to filters with ultraviolet irradiation in a Stratalinker (Stratagene, La Jolla, CA). Filters were prehybridized in 50% formamide, 6× SSPE (1× SSPE: 0.15 M sodium chloride, 0.01 M sodium phosphate, pH 7.5, 1 mM EDTA), 0.5% sodium dodecyl sulfate (SDS), 100 μg denatured salmon sperm DNA, 10× Denhardt's (1× Denhardt's: 0.01% Ficoll 400, 0.01% polyvinylpyrrolidone, 0.01% BSA) at 42°C for 2 to 6 hours. Filters were hybridized in 50% formamide, 6× SSPE, 0.5% SDS, 1× Denhardt's, 100 μg denatured salmon sperm DNA, 10% dextran sulfate with 10^{6} cts/minute/ml at 42°C for 16 hours. The 3.7 kb murine c-*kit* cDNA labeled with ^{32}P-dCTP, prepared by the random primer method, was used as a probe. Filters were washed 4× 15 minutes at room temperature in 2× SSC, 0.5% SDS and once

for 15 minutes at room temperature in 0.1× SSC, 0.5% SDS. The final wash was in 0.1× SSC, 0.5% SDS at 42°C for 30 minutes.

Pulse field gel electrophoresis (PFGE)

Samples for PFGE were prepared as described (Zelenetz et al., 1991). Briefly, spleen cells were purified on a Ficoll-Hypaque density gradient (Pharmacia). Cells were resuspended in $T_{10}E_{100}$ (10 mM Tris, pH, 100 mM EDTA) at 3.36×10^7 cells/ml and mixed with an equal volume of molten agarose solution (2% InCert agarose (FMC, Rockland, ME) in $T_{10}E_{100}$) cooled to 42°C. Aliquots (250 μl) of the molten agarose-cell suspension were placed in plug molds (BioRad, Richmond, CA) and allowed to solidify at 4°C. Plugs were then suspended in 10 ml of $T_{10}E_{100}$ containing 1% N-lauryl sarcosine (Sigma, St Louis, MO) and 200 μg/ml Proteinase K (Boehringer-Mannheim, Indianapolis, IN) and incubated at 55°C for 16 hours. Plugs were then equilibrated with a large volume of TE to remove the detergent. Next, the plugs were equilibrated in TE containing 1 mM phenylmethylsulfonyl fluoride (Sigma) to inactivate the Proteinase K. Finally the plugs were extensively washed in TE and stored in $T_{10}E_{100}$ at 4°C. For analysis, the plugs were divided into 6 parts of approximately 40 μl, with each 40 μl containing 4-5 μg of DNA. Before restriction with restriction endonucleases the 40 μl plugs were equilibrated for 30 minutes at room temperature (repeated twice) in the restriction buffer provided by the manufacturer. The buffer was replaced by fresh buffer containing 50 U of restriction endonuclease and the enzyme was allowed to diffuse into the plug for 4 hours on ice before incubation at 37°C for 16 hours. The plug was transferred into a well in the pulsed-field gel and sealed with agarose.

PFGE was performed in a contour-clamped homogenous electric field (CHEF) apparatus. Electrophoresis was performed at 14°C in 0.5× TBE with a pulse time (T_p) of 1 minute to 2 minutes in an electric field of 6 V/cm for 21 hours. *Saccharomyces cerevisiae* chromosomes (BioRad) were used for size marker.

DNA transfer was the same as for the conventional gels but the times were as follows: depurination: 5 minutes, denaturation: 30 minutes, neutralization: 30 minutes, transfer: 4 hours. Conditions for prehybridization, hybridization and washing of the filters were the same as for the Southern blots. A *Pvu*II-*Sac*I c-*kit* fragment (−617 to +37, 5′ exon probe) was used as a probe.

In situ hybridization

In situ hybridization protocols were essentially as described (Manova et al., 1990). Briefly, dissected embryos were fixed in 4% paraformaldehyde in 0.1 M phosphate buffer pH 7 overnight, washed, dehydrated and embedded in paraffin (Tissue Prep). Sections 5 μm thick were mounted on poly-L-lysine-coated slides and dried. ^{35}S-labeled antisense and sense riboprobes were synthesized with SP6 and T7 polymerase, respectively, and hydrolysed in mild alkali to a length of 100-200 nucleotides. The c-*kit* probe was transcribed from a 3.6 kb insert including the entire coding region. The KL probe was synthesized from the pcDNA1-KL plasmid which contains the entire KL coding sequence after cleavage with *Bgl*II. The slides were hydrated, postfixed in paraformaldehyde followed by treatment with proteinase K and acetic anhydride and prehybridized. Slides were hybridized overnight at 65°C in a moist chamber using 0.3 M NaCl and 60% formamide in the mix and a probe concentration of 0.25 ng/μl. Slides were washed as described except that the RNase conditions were 50 μg/ml in 0.3 M NaCl, 0.01 M Tris pH 8, 1 mM EDTA, for 30 minutes at 37°C. Slides were dipped in NTB2 emulsion, exposed for 1-2 weeks, developed and stained with eosin and hematoxylin according to standard techniques.

Immunohistochemistry

Antibody to the c-*kit* receptor was raised in rabbits by immunization with recombinant vaccinia modified to express the entire c-*kit* protein (Nocka et al., 1990a). Antisera and control rabbit serum were partially purified by DEAE Affi-gel Blue (BioRad) chromatography to enrich for immunoglobulins. Column fractions of the c-*kit* anti-sera were used at dilutions of 1:50. Dissected embryos were washed twice in 0.1 M sodium phosphate buffer (pH 7), some were fixed in 2-4% buffered paraformaldehyde and embedded in O.C.T. (Tissue Tek). Cryostat sections were cut at 10 μm and stained with the Vectastain Elite ABC kit (Vector Laboratories). The manufacturer's instructions for the procedure were followed except that the quenching of endogenous peroxidase was carried out in 0.1% H_2O_2 in phosphate-buffered saline (PBS) for 15 minutes, and incubation in 10% normal goat serum in PBS with 2% BSA for 30 minutes was included as a blocking agent for the secondary antibody, as well as an extra step to block nonspecific binding using the avidin/biotin blocking kit from Vector Laboratories. Some sections were counter-stained with Harris' hematoxylin, before dehydration and mounting in Permount.

RESULTS

Determination of c-kit RNA expression in tissues of adult W^{sh}/W^{sh} mice: lack of c-kit expression in mast cells and lung

In order to determine if W^{sh} is a c-*kit* expression mutation, we first investigated c-*kit* mRNA levels in tissues of adult W^{sh}/W^{sh} mice by RNA blot analysis. W^{sh} homozygous mice lack mast cells in their skin and intestine. In *W* mutant mice, mast cell progenitors are present in the bone marrow and, from these, mature mast cells can be grown in vitro in the presence of interleukin-3 (IL-3) (Yung and Moore, 1982; Nocka et al., 1990c). W^{sh}/W^{sh} mast cells were derived from bone marrow of homozygous mutant animals. After 4 weeks in culture, a pure population of bone-marrow-derived mast cells containing toluidine-blue-stained granules and indistinguishable from normal bone-marrow-derived mast cells were obtained (Fig. 1B) and RNA was extracted for RNA blot analysis. W^{sh}/W^{sh} mast cells lack c-*kit* RNA transcripts in contrast to the high levels seen in +/+ mast cells (Fig. 1A). Thus the absence of mast cells in homozygous mutant mice probably results from the lack of c-*kit* expression in mast cells. Consistent with the lack of effect of the W^{sh} mutation on fertility, c-*kit* RNA expression in W^{sh}/W^{sh} testis was normal (Fig. 1A). Moreover, in brain, a tissue not known to be affected by *W* mutations, c-*kit* RNA expression was normal, while W^{sh}/W^{sh} lung lacked c-*kit* transcripts (Fig. 1A). These results indicate that the W^{sh} mutation affects c-*kit* RNA expression in a tissue-specific manner.

Characterization of c-kit RNA and protein expression during embryonic development of W^{sh}/W^{sh} mice

In order to investigate tissue-specific effects of the W^{sh} mutation on c-*kit* expression during embryogenesis with an emphasis on melanogenesis, we characterized c-*kit* RNA and protein expression at various stages of development in mutant mice by in situ hybridization and immunohistochemistry.

Embryonic day 13½: Absence of presumptive melanoblasts and lack of c-kit expression in digestive tract and lung

At E13½ melanoblasts have reached the ventral part of the body at all levels along the anterior-posterior axis and some have migrated into the epidermis. In normal embryos, melanoblasts of this stage express the c-*kit* proto-oncogene (Fig. 2A,E: cross section at the level of the lung, panel C and G: slightly more caudal cross section at level of testis). In W^{sh}/W^{sh} embryos, however, no c-*kit*-positive cells were detected in the skin (Fig. 2B,F and D,H: cross sections at the same level as sections in Fig. 2A,E and C,G, respectively). Thus, in E13½ W^{sh}/W^{sh} embryos, the melanoblasts are either absent or they are present but do not express c-*kit* (see later). At E13½ the fetal liver is the major site of fetal hematopoiesis. We found that, in W^{sh}/W^{sh} embryos, the fetal liver shows normal c-*kit* expression (data not shown). Since homozygous W^{sh} mice are not anemic, this result is in accordance with the phenotype. Also in agreement with the W^{sh} phenotype, we found that the testis of E13½ W^{sh}/W^{sh} embryos express c-*kit* (Fig. 2I,J). In normal embryos, mesenchymal cells around the bronchi of the developing lung express c-*kit* at E13½ (Fig. 2A,E). Consistent with the northern blot results of RNA from adult tissues, these cells do not express c-*kit* in E13½ W^{sh}/W^{sh} embryos (Fig. 2F). In addition, there is no c-*kit* expression in the mesenchymal layer of the digestive tract in E13½ W^{sh}/W^{sh} embryos (Fig. 2, compare panels I and J: W^{sh}/W^{sh} with panels K and L: +/+). c-*kit* expression in W^{sh}/W^{sh} embryos is normal in most other tissues, including the brain (tel-, met- and myelencephalon), trigeminal ganglion, endolymphatic sac and duct, thymus, pancreas, kidney, neural tube, dorsal root and sympathetic ganglia (data not shown). Most of the results on c-*kit* expression have been confirmed at the protein level using c-*kit* antibody (data not shown).

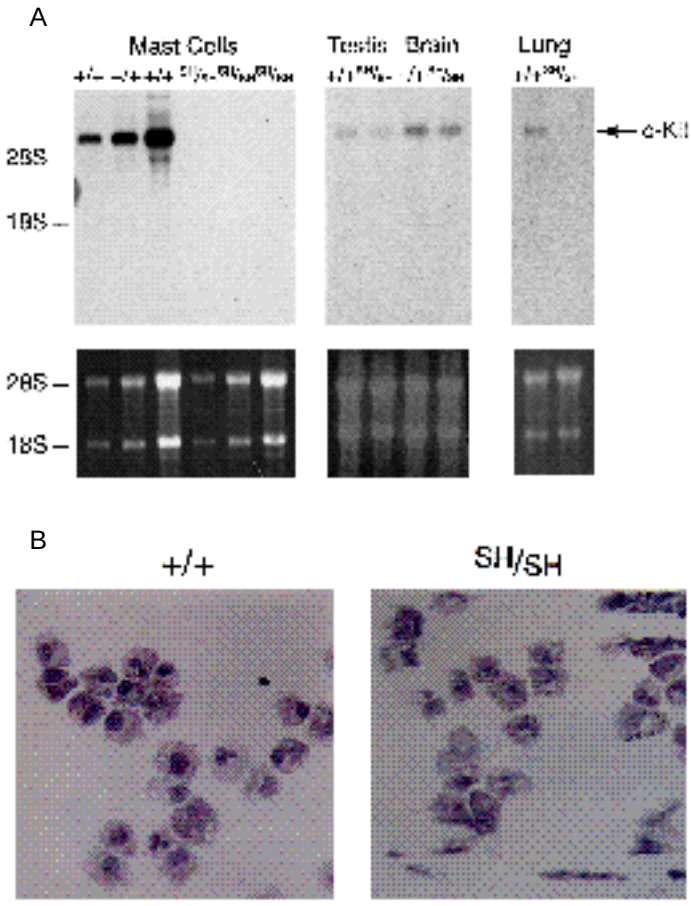

Fig. 1. (A) Expression of c-*kit* RNA in tissues from adult normal and W^{sh}/W^{sh} mice. Total RNA was prepared from bone-marrow-derived mast cells, testis, brain and lung and analyzed by blot hybridization with a c-*kit* DNA probe. The amounts of RNA samples were: mast cells, 1 μg, 2 μg and 5 μg; testis, brain and lung, 15 μg. The migration of the 5.5 kb c-*kit* mRNA is indicated by an arrow. (B) Bright-field photomicrographs of toluidine blue-stained W^{sh}/W^{sh} and normal bone-marrow-derived mast cells.

Embryonic day 10½-11½: inappropriate c-kit RNA and protein expression in the dermatome of somites, the mesenchyme around the otic vesicle and the floor plate of the neural tube

In situ hybridization of sections of E10½ W^{sh}/W^{sh} embryos gave the most surprising result. We found that in homozygous W^{sh} embryos, c-*kit* RNA is expressed ectopically in the floorplate of the neural tube extending anteriorly to the floorplate of the myelencephalon (Fig. 3B,E,H,K), in the mesenchyme around the otic vesicle (Fig. 3B,E) and in the dermatome of the somites (Fig. 3H,K). Expression in the dermatome was found in all somites along the anterior-posterior axis, except the most recently formed caudal somites. Sections of +/+ embryos hybridized with a c-*kit* probe show that c-*kit* is not expressed in these structures normally (Fig. 3A,D,G,J). In contrast, normal embryos of this stage express the kit-ligand in the floorplate, the mesenchyme around the otic vesicle and the dermatome (Fig. 3C,F,I,L).

Ectopic c-*kit* expression in W^{sh}/W^{sh} embryos did not affect kit-ligand expression. In Fig. 4A,B, similar kit-ligand expression was observed in the dermatome and the floorplate of W^{sh}/W^{sh} embryos as in +/+ embryos. Importantly, c-*kit* and kit-ligand are expressed in essentially every cell in these structures (Fig. 4C-F) indicating that kit-ligand and c-*kit* are coexpressed in floorplate and dermatomal cells in W^{sh}/W^{sh} embryos. The ectopic c-*kit* expression in W^{sh}/W^{sh} embryos may provide an explanation for the defect in melanogenesis in W^{sh} mutant mice (see discussion).

Next, we performed immunohistochemical staining in order to determine whether c-*kit* protein is also present in these structures. The results show that c-*kit* protein is present in the floorplate of E10½ W^{sh}/W^{sh} embryos (Fig. 5B), while absent in the wild-type embryo (Fig. 5A). No staining was seen in W^{sh}/W^{sh} control sections treated with preimmune serum (Fig. 5C). In E11½ W^{sh}/W^{sh} embryos c-*kit* protein was found in the mesenchyme around the otic vesicle (Fig. 6A) and in the dermatome (Fig. 6E-G). As expected, in the wild-type embryo, these structures are negative (Fig. 6B,D). Interestingly, in E11½ W^{sh}/W^{sh} embryos, the floorplate no longer expresses c-*kit* protein (Fig. 6A,E); thus this ectopic c-*kit* expression in W^{sh}/W^{sh} embryos is transient.

No c-*kit*-positive cells were seen in the skin of E13½ W^{sh} homozygous embryos (see above). Therefore, we next determined whether melanoblasts are present in W^{sh}/W^{sh}

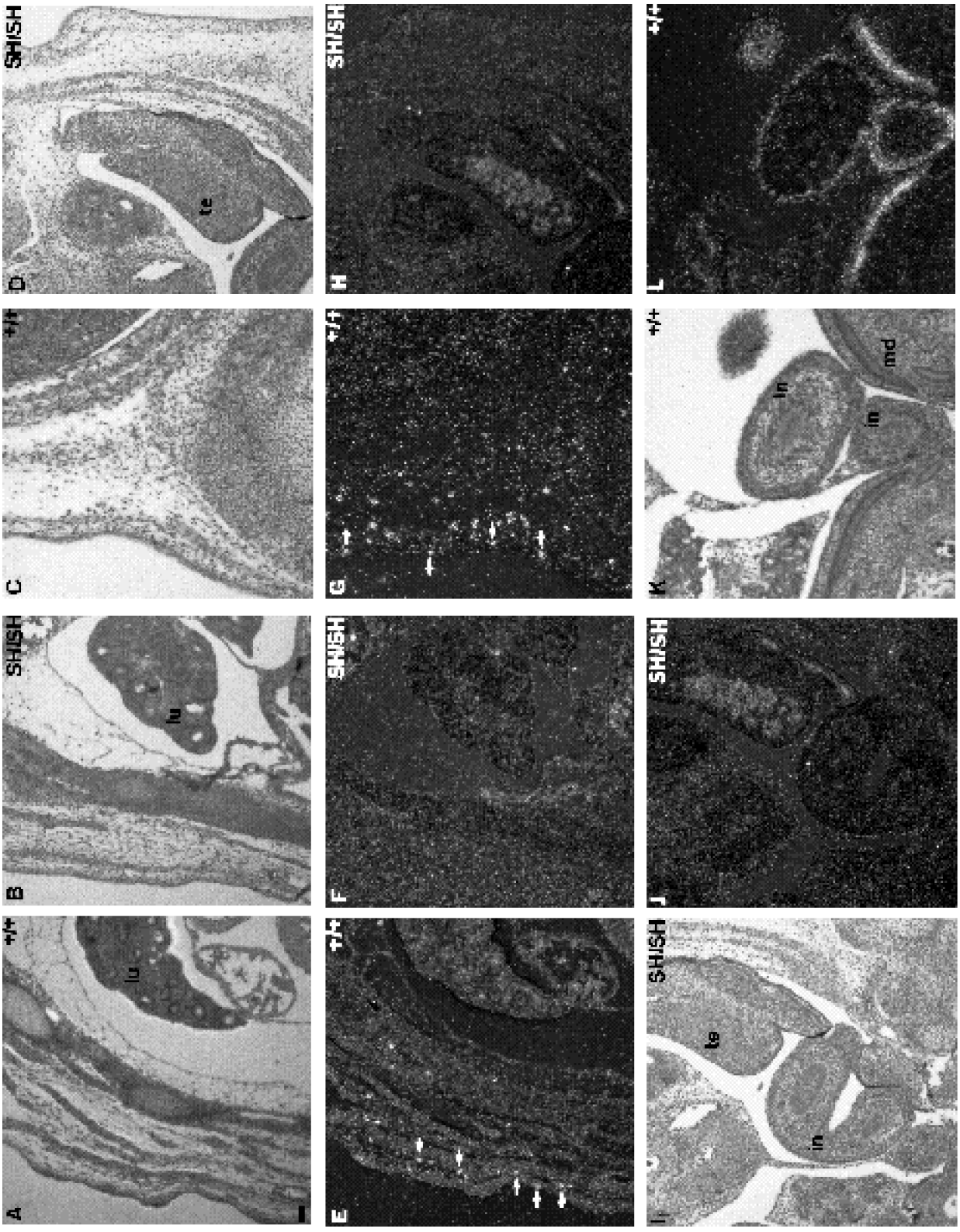

Fig. 2. In situ hybridization analysis of *c-kit* RNA expression in normal and W^{sh}/W^{sh} E13½ embryos. (A,C,K) Bright-field images of cross sections of normal embryos. (E,G,L) Dark-field images of panels A,C and K, respectively. (B,D,I) Bright-field images of cross sections of W^{sh}/W^{sh} embryos. (F,H,J) Dark-field images of B,D and I, respectively. Arrows in E and G point to some *c-kit*-positive cells in skin of normal embryos. Abbreviations: in, intestine; lu, lung; md, mesonephric duct; te, testis. Scale bar in A, 40 μm for A-L.

embryos at E10½ and E11½, a time when c-*kit*-expressing melanoblasts are normally found at the level of the somites in the trunk region (Fig. 7A,B). In E10½ W^{sh}/W^{sh} embryos, c-*kit*-positive melanoblasts were detected in low numbers, but comparable to those in +/+ embryos (Fig. 7C,F, sections at the level of the hindlimb). In E11½ W^{sh}/W^{sh} embryos, c-*kit*-positive melanoblasts were still seen but their numbers were already reduced compared to those in +/+ embryos. In Fig. 7D,F, c-*kit*-positive cells are seen migrating over the dermatome and, in Fig. 7E, c-*kit* protein expression in the dermatome is obvious. Therefore, in E10½ W^{sh}/W^{sh} embryos, melanoblasts express c-*kit* gene products and the absence of melanoblasts at later stages may be the result of ectopic c-*kit* expression in the dermatome.

Melanocyte progenitors in +/+ and W^{sh}/+ embryos: graded distribution is reduced in W^{sh}/+ embryos along the body axis

To gain further insight into the timing and mechanism of disappearance of melanoblasts in W^{sh} mutant embryos, a

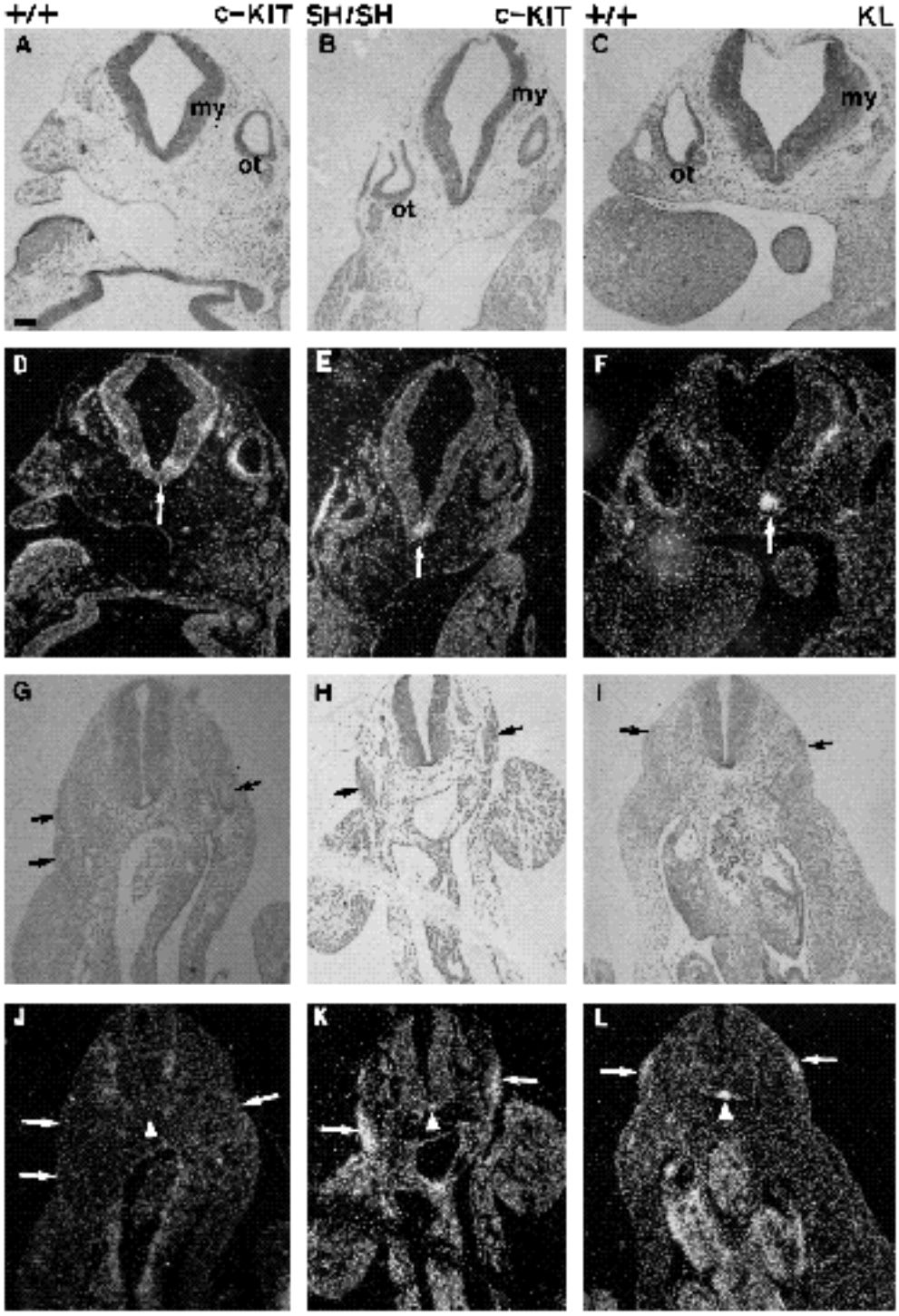

Fig. 3. Expression of c-*kit* and KL RNA in normal and E10½ W^{sh}/W^{sh} embryos. (A,G) Bright-field images of cross sections of normal embryos hybridized to the c-*kit* antisense probe. (D,J) Dark-field images of panels A and G, respectively. (B,H) Bright-field images of cross sections of W^{sh}/W^{sh} embryos hybridized to the c-*kit* antisense probe. (E,K) Dark-field images of panels B and H, respectively. (C,I) Bright-field images of cross sections of ICR×CB6F1 embryos hybridized to the KL antisense probe. (F,L) Dark-field images of panels C and I, respectively. Arrows in panels D-F point to the floorplate and arrows in panels G-L point to the somites. Abbreviations: my, myelencephalon; ot, otic vesicle. Scale bar in panel A, 75 μm for panels A-L.

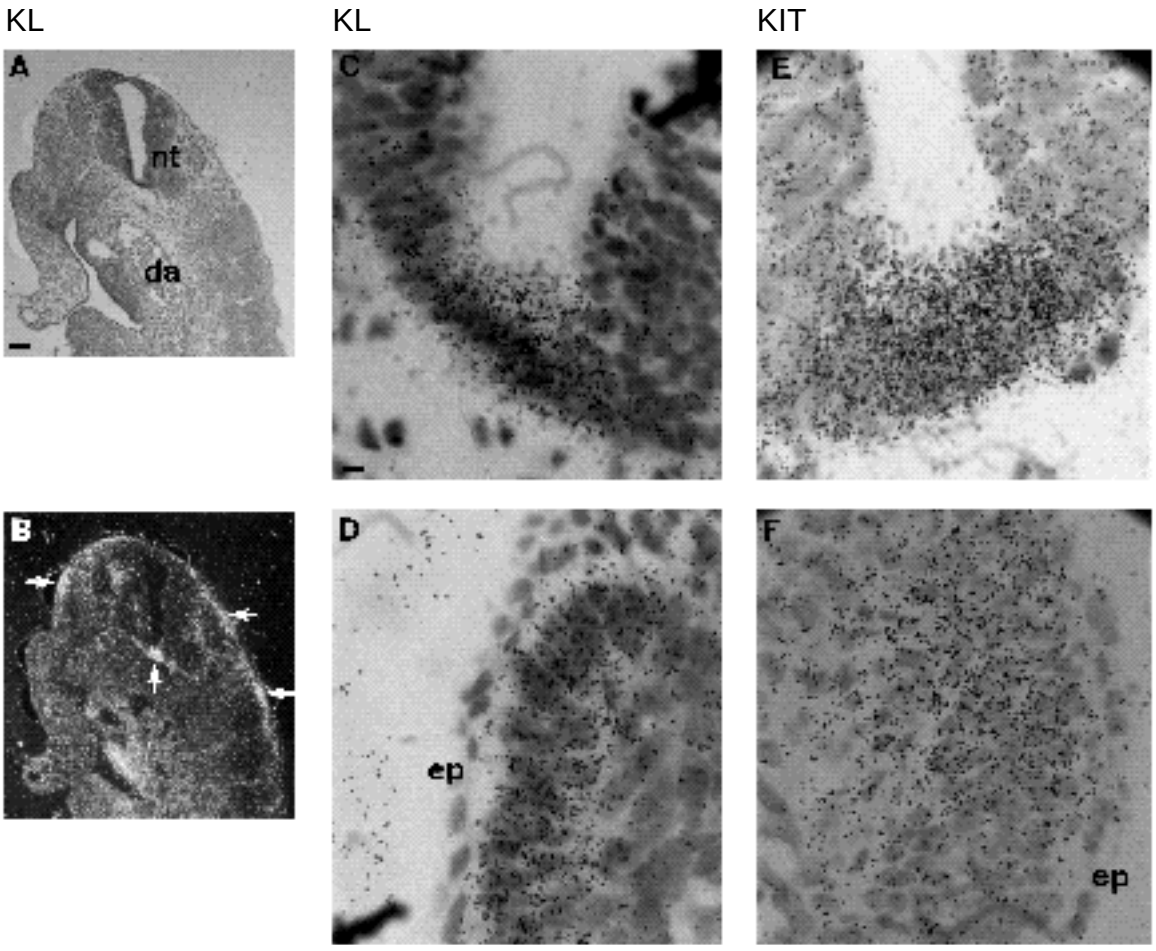

Fig. 4. Co-expression of KL and c-kit RNA in E10½ W^{sh}/W^{sh} embryos. Bright-field image (A) and dark-field image (B) of sagittal section of W^{sh}/W^{sh} embryo hybridized to the KL antisense probe. White arrows in B point to labeled somites and floorplate. (C,D) Higher magnification of the floorplate and the dermatome of one somite shown in A and B. (E) Higher magnification of the floorplate of the neural tube shown in Fig. 3B and E, hybridized to the c-*kit* antisense probe. (F) Higher magnification of the dermatome of a somite, hybridized to the c-*kit* antisense probe. Abbreviations: da, dorsal aorta; ep, epidermis; nt, neural tube. Scale bar in A, 75 μm for A and B. Scale bar in C, 20 μm for C-F.

detailed analysis of the distribution of melanoblasts in E13½ +/+ and W^{sh}/+ embryos was undertaken. Since wild-type melanoblasts express c-*kit* from E10½ onwards (Manova and Bachvarova, 1991), in W^{sh}/+ embryos unlike in homozygous mutant embryos, an absence of c-*kit*-positive cells indicates an absence of melanoblasts. E13½ wild-type and heterozygous embryos were serially sectioned in sagittal and cross section orientation and regularly spaced sections processed for immunohistochemistry using the anti-c-*kit* serum. At E13½ melanoblasts are located in the dermis and the epidermis, but some c-*kit*-positive mast cell progenitors may also be present in the dermis (Hayashi et al., 1985). Therefore, the distribution of melanoblasts was assessed by counting only c-*kit*-positive cells in the epidermis. Examples of stained melanoblasts in different regions of these embryos are shown in Fig. 8. Little staining was seen in control sections stained with preimmune serum (not shown). Note continued ectopic expression of c-*kit* in the dermis of W^{sh}/+ embryos (also in E13½ W^{sh}/W^{sh} embryos, not shown), which extends to the ventral midline at this stage. A quantitative representation of the results was obtained by plotting epidermal melanoblasts in sagittal sections (Fig. 9A) or by plotting the density of cells in the dorsal half of cross sections (Fig. 9B). The results indicate that, in wild-type embryos, melanoblasts are distributed in a graded fashion with maximal numbers in the rostral and caudal regions and a minimum in the lumbar region. In W^{sh}/+ embryos, the density of the melanoblasts is reduced throughout resulting in a virtual absence in the trunk region.

At E11½ melanoblasts are already distributed at varying densities along the body axis with a minimum in the lumbar region and their number is reduced in W^{sh}/+ embryos (Fig. 10). Mast cells essentially are absent from the skin at this age (Hayashi et al., 1985). In W^{sh}/+ embryos, as in W^{sh}/W^{sh} embryos, regions of head mesenchyme, particularly around the otic vesicle, and all dermatomes along the axis of the embryo expressed c-*kit* at similar levels. At this stage, dermis expressing c-*kit* has almost reached the ventral midline in the thoracic region. Since, melanoblasts are essentially normal in E10½ embryos (see above), these

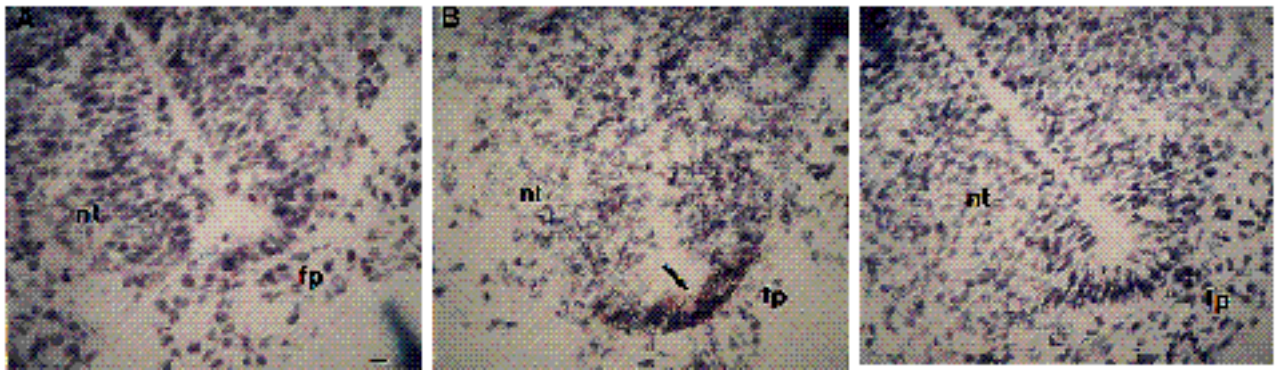

Fig. 5. Immunohistochemical analysis of c-*kit* protein expression in the floorplate of E10½ W^{sh}/W^{sh} embryos. Bright-field photomicrographs of cross sections of normal (A) and W^{sh}/W^{sh} (B) embryos stained with anti-c-*kit* antibody; arrow points to c-*kit*-positive floorplate. (C) Control section stained with preimmune serum. Abbreviations: fp, floor plate; nt, neural tube. Scale bar in A, 30 μm for A-C.

results establish that the melanocyte defect in $W^{sh}/+$ embryos, the "sash", occurs between E10½ and E13½.

Analysis of W^{sh} chromosomal DNA

In order to determine whether the W^{sh} mutation arose as a result of a DNA rearrangement or deletion, we investigated the c-*kit* gene in W^{sh} chromosomal DNA using conventional and pulsed-field gel electrophoresis (PFGE) DNA blots. Southern blot analysis of DNA from normal and W^{sh}/W^{sh} mice shown in Fig. 11A using either the c-*kit* cDNA or sequences including the first exon of the c-*kit* gene (not shown) as probes revealed no differences between the mutant and the normal DNA suggesting that the c-*kit* gene in the W^{sh} DNA is unaltered. However, analysis of blots obtained after resolution of megabase DNA by PFGE, digested with the restriction enzymes *Not*I, *Nru*I and *Nar*I and hybridization with a c-*kit* probe revealed W^{sh} DNA fragments of a reduced size with all three enzymes (Fig. 11B). Since the W^{sh} mutation arose in F_1 C3H/HeH × 101/H mice, we also analyzed DNA from C3H/HeJ and 101.

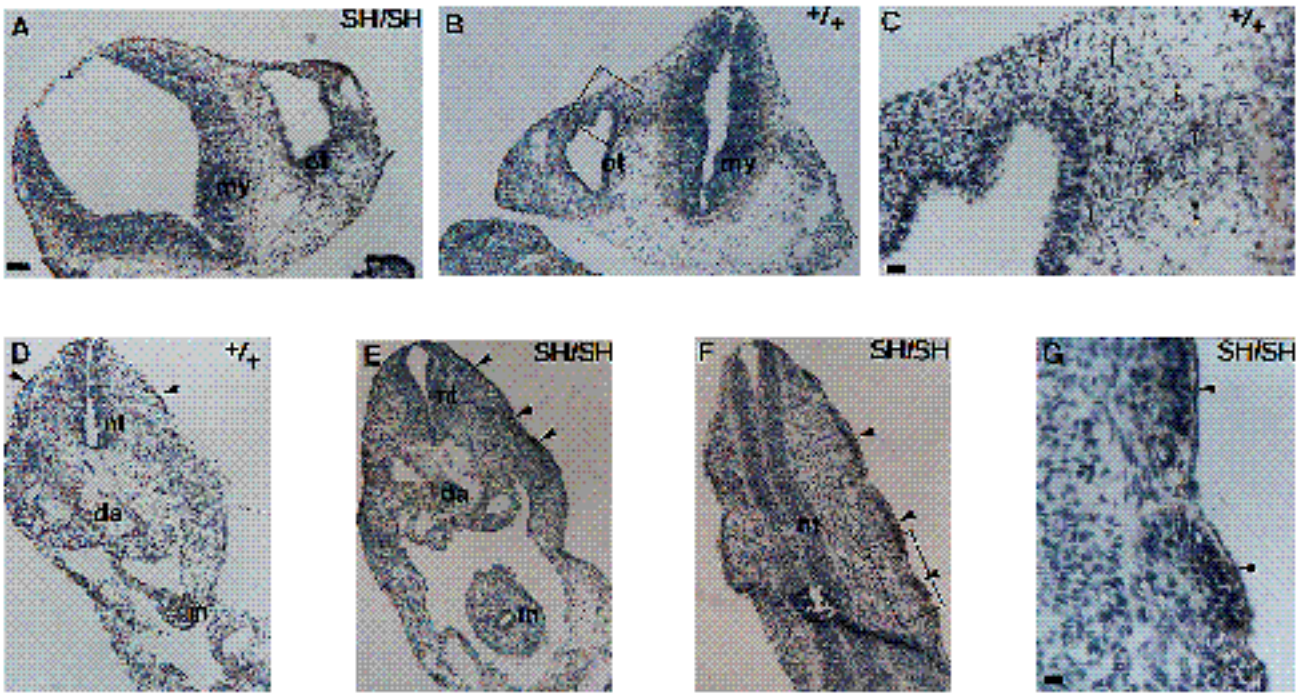

Fig. 6. Expression of c-*kit* protein in sections of E11½ normal and W^{sh}/W^{sh} embryos stained with anti-c-*kit* antibody. (A,E,F,G) W^{sh}/W^{sh} embryos; (G) higher magnification of the boxed region in F. (B,C,D) Normal embryos. (C) Higher magnification of the boxed region in B. Arrowheads in E-G indicate labeled somites in W^{sh}/W^{sh} embryos. Arrowheads in D point to somites in +/+ embryo. Smaller arrows in C point to some scattered c-*kit*-positive cells around otic vesicle in normal embryos. Abbreviations: da, dorsal aorta; in, intestine; my, myelencephalon; nt, neural tube; ot, otic vesicle. Scale bar in panel A, 75 μm for A,B,D,E and F. Scale bar in C, 40 μm. Scale bar in G, 30 μm.

Digestion of DNA from C3H/HeJ, 101 and C57BL/6J mice with *Not*I (Fig. 11C lanes 1,2 and 3) and *Nru*I (Fig. 11C lanes 5,6 and 7) resulted in indistinguishable restriction fragments. Taken together these results suggest that the W^{sh} allele arose as a result of a deletion or a rearrangement in the vicinity of the c-*kit* gene.

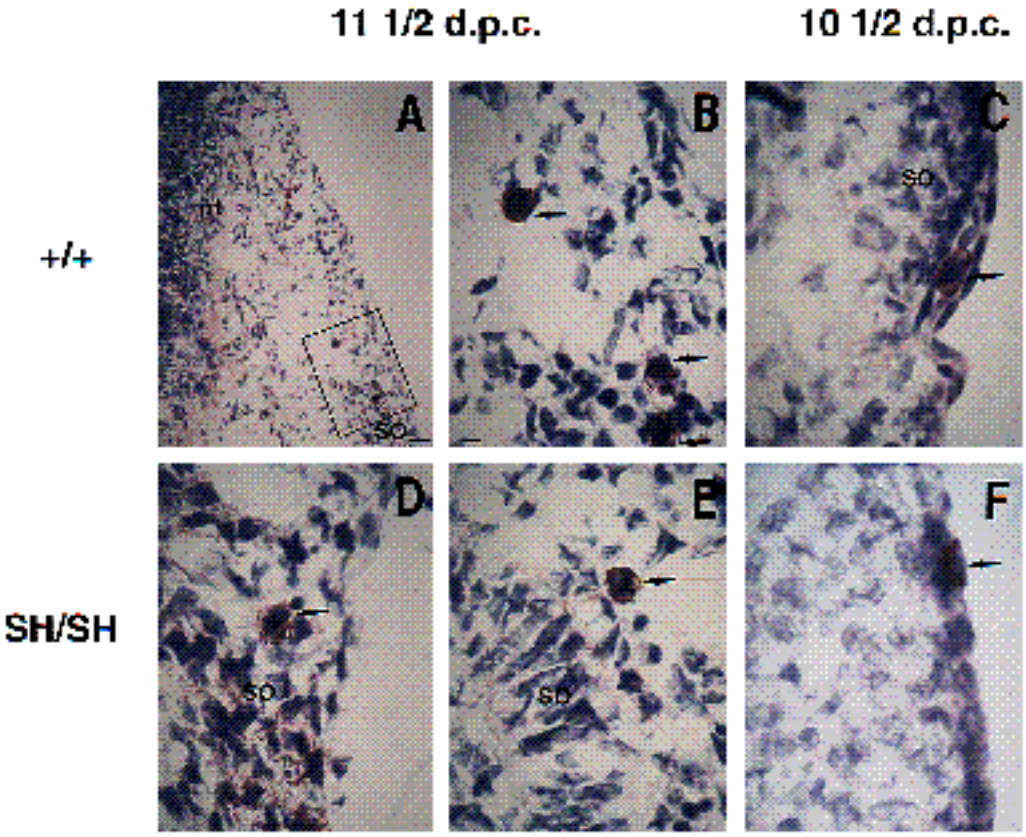

Fig. 7. Expression of c-*kit* protein in melanoblasts. Bright-field photomicrographs of cross sections of normal (A,B [E11½] and C [E10½]) and W^{sh}/W^{sh} (D,E [E11½] and F [E10½]) embryos stained with anti-c-*kit* antibody. (B) Higher magnification of boxed region in A. Arrows in B-F point to labeled melanoblasts. Abbreviations: nt, neural tube; so, somite. Scale bar in A, 40 μm. Scale bar in B, 20 μm for B-F.

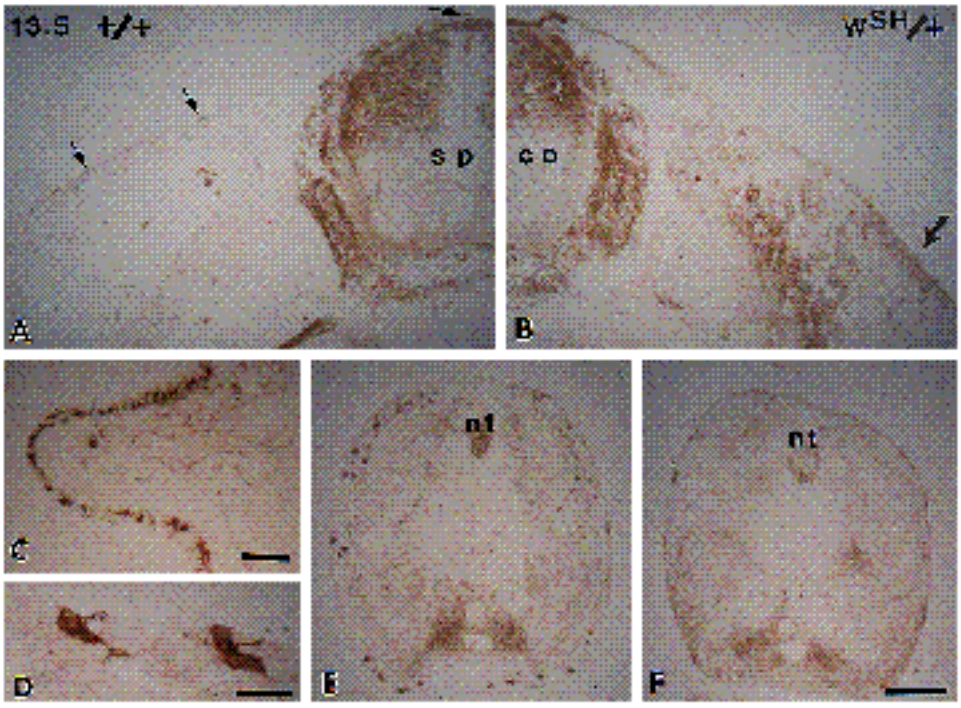

Fig. 8. Expression of c-*kit* protein in E13½ +/+ and W^{sh}/+ embryos. Sections of C57BL/6J and W^{sh}/+ 13.5 day embryos stained with anti-c-kit antibody. (A) Cross section of C57BL/6J embryo (+/+) in the lower thoracic region. Arrows indicate three of the several stained cells in the epidermis. (B) Corresponding section of a W^{sh}/+ embryo. Arrow indicates stained dermis. Deeper mesenchyme is also stained. There are few or no stained cells in the epidermis. (C) Section of the ear pinna of a +/+ embryo. Note high density of stained cells in the epidermis. Scale bar, 100 μm. (D) High magnification view of two presumptive melanoblasts in the epidermis of the thoracic region. Scale bar, 20 μm. (E) Cross section of the proximal tail of a +/+ embryo. (F) Corresponding section of the tail of a W^{sh}/+ embryo with much lower density of stained cells in the epidermis and dermis. Scale bar, 200 μm for A,B,E and F. sp co, spinal cord; nt, neural tube.

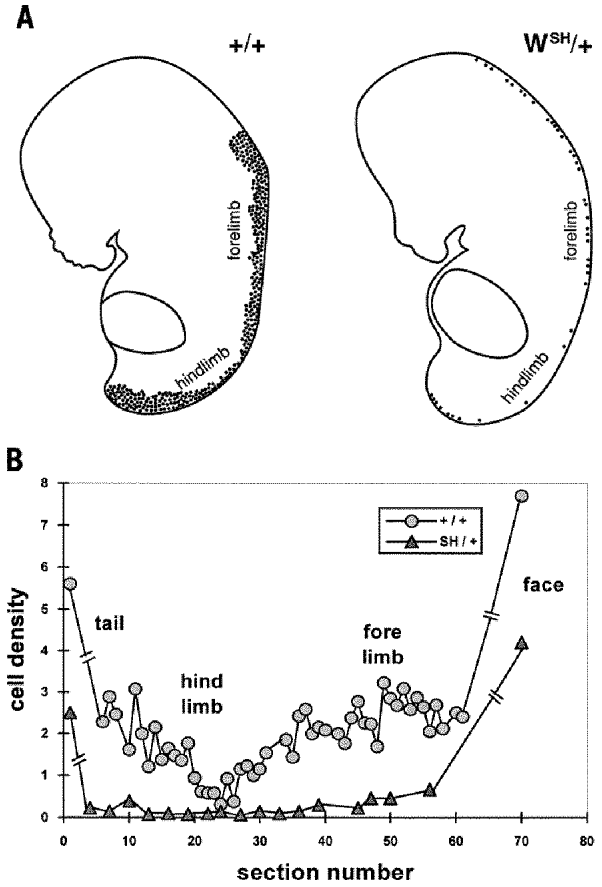

Fig. 9. Density of c-*kit*-positive cells (presumed melanoblasts) in +/+ and W^{sh}/+ E13½ day embryos. (A) Density of c-*kit*-positive cells along the cranial-caudal axis assessed on sagittal sections. Stained cell bodies or processes within the epidermis were located in six parasagittal sections from +/+ and W^{sh}/+ embryos and their positions plotted on a 22× tracing of one composite section. Only cells on the dorsal surface from the neck down were plotted. (B) Density of c-*kit*-positive cells along the cranial-caudal axis assessed on cross sections. Epidermal c-*kit*-positive cell bodies or processes in the dorsal half of cross sections were counted, the relative density computed and values plotted on an arbitrary scale for sections numbered from the caudal end. The data for face and proximal tail were taken from both cross and sagittal sections, and plotted at an arbitrary position at each end. The face consisted of the region around the eyes and the dorsal surface of the snout.

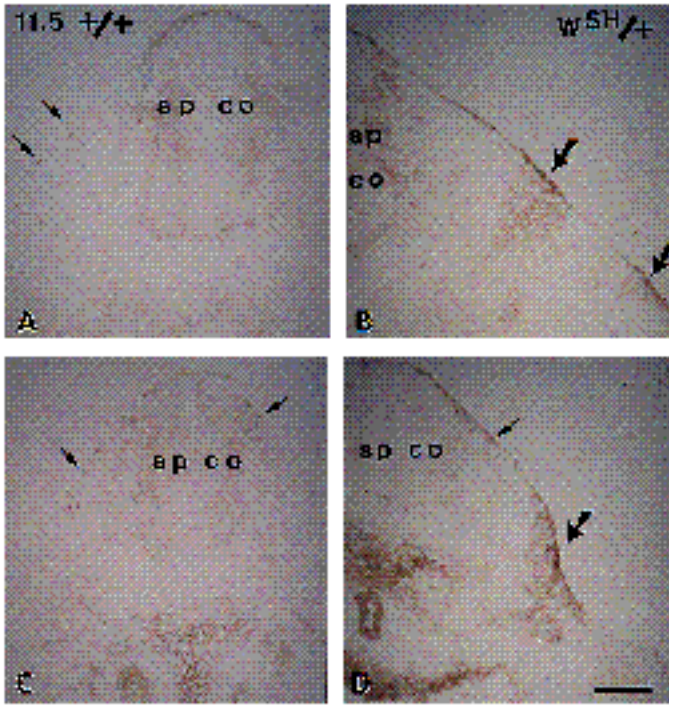

Fig. 10. Expression of c-*kit* protein in E11½ +/+ and W^{sh}/+ embryos. Sections of E11½ day embryos were stained with anti-c-*kit* antibody. (A) Approximate cross section of a +/+ embryo in the lower thoracic region. Arrows indicate two of the several stained cells in dermis and epidermis. (B) Corresponding section of a W^{sh}/+ embryo. Arrows indicate stained dermatomes. Few or no stained melanoblasts are seen in the dermis or epidermis. (C) Section caudal to the hind limb. Arrows indicate two quite abundantly stained cells in the dermis and epidermis. (D) Corresponding section of a W^{sh}/+ embryo. Large arrow indicates stained dermatome. The +/+ embryo sections were processed in a separate experiment and the c-*kit*-positive cells are stained more lightly. Small arrow indicates one of several stained cells in the dermis and epidermis. Scale bar, 200 μm for all panels. sp co, spinal cord.

DISCUSSION

The non-parallel display of mutant characteristics in mice containing the W^{sh} allele suggested that the phenotypes of this mutation could result from tissue-specific effects on c-*kit* transcription or post-transcriptional processing. We therefore characterized c-*kit* expression patterns in various tissues and cell types of homozygous mutant mice at various stages of development. Our experiments show that several tissues that normally express c-*kit* do not express c-*kit* in W^{sh}/W^{sh} mice; they include bone-marrow-derived mast cells of adult W^{sh}/W^{sh} mice, adult and fetal lung and the digestive tract at embryonic day 13½. c-*kit* expression is not affected in most other adult and fetal tissues in W^{sh}/W^{sh} mice. E10½ W^{sh}/W^{sh} embryos have normal numbers of c-*kit*-expressing melanoblasts but at E13½ the homozygous and heterozygous mutant embryos lack c-*kit*-positive cells in the skin or have proportionally reduced numbers, respectively. A surprising but major finding was the expression of c-*kit* in mutant 10½-11½ day embryos in some tissues and cell types that do not normally express c-*kit* but do express the kit-ligand, i.e. the dermatome of the somites, the mesenchyme around the otic vesicle and the floorplate of the neural tube. The inappropriate c-*kit* expression does not affect kit-ligand expression in homozygous mutant embryos. Furthermore, molecular analysis of W^{sh} chromosomal DNA revealed a deletion or rearrangement in the vicinity of the c-*kit* gene. These results provide possible explanations for the phenotypes of homozygous and heterozygous W^{sh} mice, and they have implications for the transcriptional control of the c-*kit* proto-oncogene.

The W^{sh} mutation differs from other *W* mutations in that only mast cells and melanocytes are affected, whereas germ cells and erythrocytes areaffected only in minor ways (Lyon

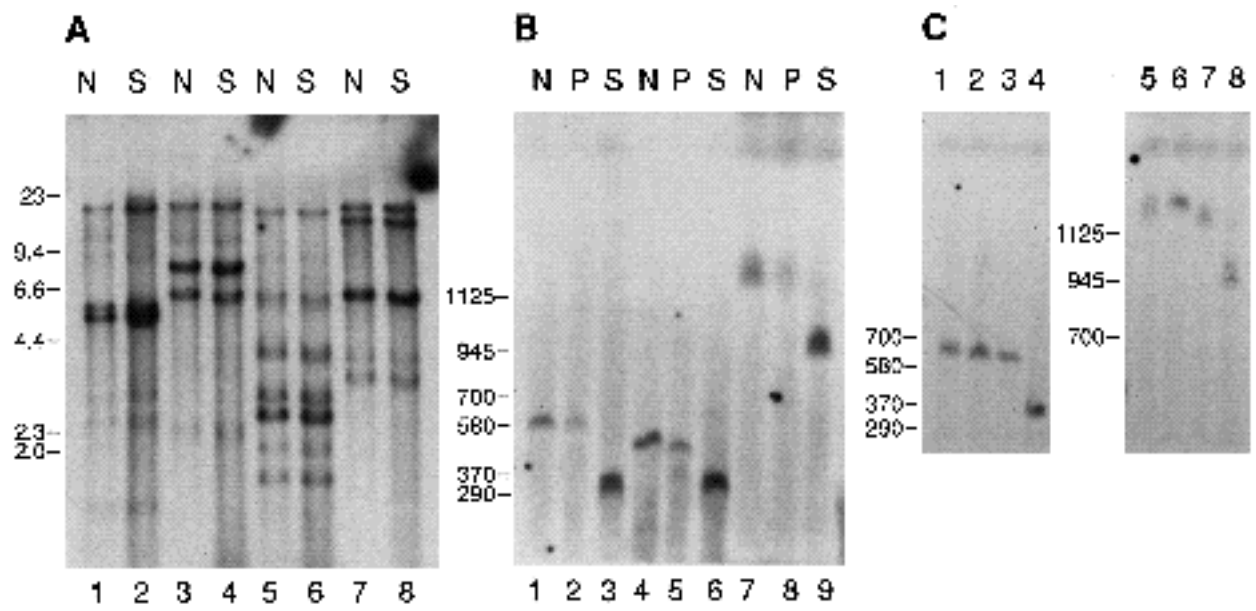

Fig. 11. Analysis of c-*kit* locus in DNA from W^{sh}/W^{sh} and normal mice. (A) Southern blot analysis: DNA from W^{sh}/W^{sh} (S) and C57BL/6J (N) mice was digested with the enzymes *Eco*RI (lanes 1 and 2), *Bam*HI (lanes 3 and 4), *Hin*dIII (lanes 5 and 6) and *Sac*I (lanes 7 and 8), fractionated by electrophoresis in a 0.8% agarose gel and analyzed by blot hybridization with a c-*kit* DNA probe (3.6 kb cDNA probe). Migration of lambda DNA size markers is indicated. (B,C) Pulsed field gel electrophoresis (PFGE). (B) DNA from spleen cells of W^{sh}/W^{sh} (S), *Ph*/+ (P) and C57BL/6J (N) mice was digested with the enzymes *Not*I (lanes 1, 2 and 3), *Nar*I (lanes 4, 5 and 6) and *Nru*I (lanes 7, 8 and 9) and (C) DNA from C3H/HeJ, 101, C57BL/6J and W^{sh}/W^{sh} mice was digested with *Not*I (lanes 1, 2, 3 and 4) and *Nru*I (lanes 5, 6, 7 and 8). PFGE was performed in a CHEF apparatus at 14°C in 0.5× TBE with a pulse time (T_p) of 1 minute to 2 minutes in an electric field of 6 V/cm for 21 hours. Transfer of the fractionated DNA to a membrane and hybridization with the 5′ exon c-*kit* probe was as for Southern blots. Migration of *Saccharomyces cerevisiae* chromosomes as size markers is indicated.

and Glenister, 1982; Stevens and Loutit, 1982). These characteristics can be explained by the normal expression of c-*kit* in fetal liver and testis of W^{sh} mice and the lack of c-*kit* expression in mast cells. Recently, it has also been shown that CFU-S from bone marrow of W^{sh}/W^{sh} animals are severely reduced in number (Tono et al., 1992), possibly due to mis-regulated c-*kit* expression in the hematopoietic stem cell hierarchy.

The inappropriate c-*kit* expression in the dermatome of E10½ and E11½ mutant embryos is an important feature of the W^{sh} mutation, which may provide an explanation for the pigmentation defect in mutant mice. We propose that inappropriate expression of c-*kit* receptor in the dermatome of W^{sh}/W^{sh} mice may sequester (bind and neutralize) kit-ligand. As a result the amount available for c-*kit*-expressing melanoblasts migrating over the dermatome is reduced, thus affecting their survival and/or proliferation. It is also conceivable that the co-expression of c-*kit* and its ligand results in the activation of dermatomal cells by an autocrine or paracrine mechanism and this in turn may lead to changes in the extracellular matrix. In either model, the W^{sh}/W^{sh} melanoblasts would die between day E10½ and day E13½. In support of our model is the fact that, in the trunk region, at E10½-11½, melanoblasts migrate over the somites and continue to migrate as dermatome cells spread under the ectoderm from E11½-E13½, a period that coincides with the time of inappropriate c-*kit* expression in the dermatome. Also in agreement with this paradigm, we found normal numbers of c-*kit*-expressing melanoblasts in E10½ W^{sh}/W^{sh} embryos apparently on a dorsolateral pathway, whereas in 13½ day embryos no c-*kit*-positive cells were detected in the skin. Although melanoblasts appear to express c-*kit* normally in day 10½ W^{sh}/W^{sh} embryos, our results do not preclude the possibility that c-*kit* expression in more mature melanoblasts/melanocytes is affected by the W^{sh} mutation. But the presence of small patches of pigmentation around the ears and eyes in homozygous W^{sh} mice suggests that melanocytes are normal in these mice. In agreement with this notion, melanocytes have been grown from neural crest cells of W^{sh}/W^{sh} embryos (Huszar et al., 1991).

c-*kit* is expressed in all somites and the mesenchyme near the otic vesicle of W^{sh}/W^{sh} and $W^{sh}/+$ embryos apparently in the same pattern as KL. Hence, ectopic c-*kit* expression in the dermatome may not be a sufficient explanation for a differential effect of the mutation on melanocyte development in the anterior, mid and posterior regions in $W^{sh}/+$ mice. However, in the epidermis of E13½ +/+ embryos, the melanoblasts are present in a graded distribution with high densities in the face, ear and tail, moderate densities in the shoulder and rump, and a minimal density in the lumbar region. As expected from our model, melanoblasts in $W^{sh}/+$ embryos are reduced at all levels, with very few present in the lumbar region. Therefore, the formation of the *SASH* in heterozygous mutant animals may stem from a reduction of cells in the anterior, mid level and posterior regions during embryogenesis and reflects the uneven distribution of melanoblasts in normal embryos. Several patterns of mice with coat color mutations can be explained on the basis of

general effects on melanocyte precursors and the graded melanoblast distribution that we have observed at E13½ (Charles, 1938; Silvers, 1979). Taken together these results suggest that c-*kit* is required in melanogenesis between E10½ and 13½. This is a period of substantial proliferation of melanoblasts from a sparse and quite even distribution at E10½ to a more numerous population distributed differentially over the surface at E13½.

Aggregation chimeras produced from *W/W*↔+/+ embryos have a ventral spot and blaze on the forehead similar to heterozygous *W*/+ animals (Mintz, 1974). Interestingly, W^{sh}/W^{s}↔+/+ aggregation chimeras display a pigmentation pattern similar to or more pronounced than that of heterozygous W^{sh}/+ animals (Stephenson et al., 1985), in agreement with the non-cell autonomous dominant mode of action of the W^{sh} mutation that we have proposed. By contrast, transplantation of normal neural crest cells into the amniotic cavity of E8.75-9.0 W^{sh}/W^{sh} embryos results in the formation of pigment patches in apparent contradiction to our findings (Huszar et al., 1991). However, several considerations suggest that events after transplantation may not necessarily faithfully reflect normal developmental processes: first, the neural crest cells used for transplantation were cultured prior to use and may differ from the normal melanoblasts; second, the neural crest cells can be transplanted only into E8.75-9.0 embryos, and the timing of migration of the transplanted cells therefore may differ from the normal developmental program; third, the number of transplanted cells may exceed those found in normal embryogenesis and this might affect the outcome of the experiment; and fourth, the path of migration of the transplanted cells from the site of injection in the amniotic cavity is not known and may differ from the normal situation.

The W^{sh} mutation blocks c-*kit* expression in mast cells and mesenchymal cells in the lung and the digestive tract at E13½, while expression in other tissues is normal. This suggests that c-*kit* expression in different tissues is regulated by different *cis*-acting elements and that positive regulatory elements specific for mast cells and mesenchymal cells in the lung and the digestive tract are affected by the W^{sh} mutation. Furthermore, our observation of c-*kit* expression in tissues that normally express the c-*kit* ligand implies that the regulatory region of the c-kit gene includes negative control elements which are also affected by this mutation. Our Southern blot analysis indicates no alteration of c-*kit* exon and intron sequences in the W^{sh} allele in agreement with the recent demonstration that the c-kit^{WSH} coding sequence is unaltered (Tono et al., 1992). However, the results from the pulsed-field gel electrophoresis indicate that the W^{sh} mutation involves a large deletion or rearrangement and this is in agreement with our observations that several control elements are affected by this mutation. We speculate that the deletion is upstream of the c-*kit* locus based on the following observation. The *Patch* locus encodes the PDGFRA receptor and is closely linked to the c-*kit*/*W* locus (Smith et al., 1991; Stephenson et al., 1991; Duttlinger, unpublished). Interestingly, mice heterozygous for the *Patch* mutation display the same pigmentation pattern as do W^{sh}/+ mice, while homozygous *Ph/Ph* mice die during embryonic development. The original *Patch* mutation arose as a result of a deletion that includes the entire PDGFRA receptor. The 3′-deletion endpoint, which is in juxtaposition with the 5′ end of the c-*kit* gene, is not known precisely, but it does not include c-*kit* coding sequences. Because of the similar heterozygous pigmentation phenotypes of the W^{sh} and the *Patch* mutations, it is reasonable to speculate that the pigmentation defect in *Ph*/+ mice is the result of inappropriate c-*kit* expression similar to that in W^{sh}/+ mice and that the two mutations, therefore, affect some of the same elements in the 5′ control region of the c-*kit* proto-oncogene. In agreement with these predictions, preliminary results have placed the W^{sh} alteration upstream of the c-*kit* (R. Duttlinger, unpublished). We are currently investigating the precise nature of the W^{sh} mutation, its relationship to PDGFRA and its effects on PDGFRA.

Our observation of co-expression of c-*kit* and KL in W^{sh}/W^{sh} embryos in head mesenchyme, dermatomal cells and cells of the floorplate raises the interesting possibility that mechanisms regulating their expression may be related. Thus, negative control elements might be necessary to insure that c-*kit* is not expressed in tissues normally expressing KL. Such elements may be affected by the W^{sh} mutation uncovering positive regulatory elements common to c-*kit* and KL.

We would like to thank Sandra Sanchez and Michael Angeles for help with histochemistry and in situ hybridizations, Dr Hai Nguyen for histopathology and Drs Karl Nocka, Tang Yang Chu and Ellen Pritzer for advice and stimulating discussions. This work was supported by grants from the National Institutes of Health to P. B. (R37 CA 32926) and R. F. B. (HD 06910).

REFERENCES

Besmer, P. (1991). The *kit* ligand encoded at the murine *steel* locus: a pleiotropic growth and differentiation factor. *Current Opinion in Cell Biology* **3**, 939-946.

Besmer, P., Murphy, J. E., George, P. C., Qiu, F. H., Bergold, P. J., Lederman, L., Snyder, H. W., Brodeur, D., Zuckerman, E. E. and Hardy, W. D. (1986). v-*kit*: oncogene of a new acute transforming feline retrovirus (HZ4-FeSV) - relationship with the protein kinase gene family. *Nature* **320**, 415-421.

Chabot, B., Stephenson, D. A., Chapman, V. M., Besmer, P. and Bernstein, A. (1988). The proto-oncogene c-*kit* encoding a transmembrane tyrosine kinase receptor maps to the mouse *W* locus. *Nature* **335**, 88-89.

Charles, D. R. (1938). Studies on spotting patterns. IV. Pattern variation and its developmental significance. *Genetics* **23**, 523-547.

Chirgwin, J. M., Przbyla, A. E., Macdonald, J. R. and Rutter, W. J. (1979). Isolation of biologically active Ribonucleic acid from sources enriched in ribonuclease. *Biochemistry* **18**, 5294-5299.

Copeland, N. G., Gilbert, D. J., Cho, B. C., Donovan, P. J., Jenkins, N. A., Cosman, D., Anderson, D., Lyman, S. D. and Williams, D. E. (1990). Mast cell growth factor maps near the steel locus and is deleted in a number of steel alleles. *Cell* **63**, 175-183.

Feinberg, A. P. and Vogelstein, B. (1983). A technique for radiolabelling DNA restriction fragments to high specific activity. *Anal. Biochem.* **132**, 6-13.

Geissler, E. N., McFarland, E. C. and Russell, E. S. (1981). Analysis of pleiotropism at the dominant white-spotting (*W*) locus of the house mouse: a description of ten new *W* alleles. *Genetics* **97**, 337-361.

Geissler, E. N., Ryan, M. A. and Housman, D. E. (1988). The dominant white spotting (*W*) locus of the mouse encodes the c-*kit* proto-oncogene. *Cell* **55**, 185-192.

Hayashi, C., Sonoda, T., Nakano, T., Nakayama, and Kitamura, Y. (1985). Mast-cell precursors in the Skin of Mouse Embryos and their deficiency in embryos of Sl/Sl^{d} genotype. *Dev. Biol.* **109**, 234-241.

Huszar, D., Sharpe, A. and Jaenisch, R. (1991). Migration and

proliferation of cultured neural crest cells in *W* mutant neural crest chimeras. *Development* **112**, 131-141.

LeDouarin, N. (1982) *The Neural Crest.* Cambridge, UK: Cambridge University Press.

Lehrach, H., Diamond, D., Wozney, J. M. and Boedtker, H. (1977). RNA molecular weight determination by gel electrophoresis under denaturing conditions, a critical reexamination. *Biochemistry* **16**, 4743-4756.

Lyon, M. F. and Glenister, P. H. (1982). A new allele sash (W^{sh}) at the *W*-locus and a spontaneous recessive lethal in mice. *Genet. Res.* **39**, 315-322.

Lyon, M. F. and Searle, A. G. (1989). *Genetic Variants and Strains of the Laboratory Mouse.* second edition. Oxford: Oxford University Press.

Majumder, S., Brown, K., Qiu, F. H. and Besmer, P. (1988). c-*kit* protein, a transmembrane kinase: identification in tissues and characterization. *Mol. Cell. Biol.* **8**, 4896-4903.

Manova, K., Nocka, K., Besmer, P. and Bachvarova, R. F. (1990) Gonadal expression of c-*kit* encoded at the *W* locus of the mouse. *Development* **110**, 1057-1069.

Manova, K. and Bachvarova, R. F. (1991). Expression of c-*kit* encoded at the *W* locus of mice in developing embryonic germ cells and presumptive melanoblasts. *Dev. Biol.* **146**, 312-324.

Matsui, Y., Zsebo, K. M. and Hogan, B. L. M. (1990) Embryonic expression of a haematopoietic growth factor encoded by the *Sl* locus and the ligand for c-*kit*. *Nature* **347**, 667-669.

Mayer, T. C. (1965). The development of piebald spotting in mice. *Dev. Biol.* **11**, 319-334.

Mayer, T. C. (1973). The migratory pathways of neural crest cells into the skin of mouse embryos. *Dev. Biol.* **34**, 39-46.

Mintz, B. (1974) Gene control of mammalian differentiation. *Ann. Rev. Genet.* **8**, 411-470.

Nishikawa, S., Kusakabe, M., Yoshinaga, K., Ogawa, M., Hayashi, S. -I., Kunisada, T., Era, T., Sakakura, T. and Nishikawa, S.-I. (1991). In utero manipulation of coat color formation by a monoclonal anti c-*kit* antibody: two distinct waves of c-*kit* dependency during melanogenesis. *EMBO J.* **10**, 2111-2118.

Nocka, K., Majumder, S., Chabot, B., Ray, P., Cervonne, M., Bernstein, A. and Besmer, P. (1989). Expression of c-*kit* gene products in known cellular targets of *W* mutations in normal and *W* mutant mice- Evidence for impaired c-*kit* kinase in mutant mice. *Genes Dev.* **3**, 816-826.

Nocka, K., Buck, J., Levi, E. and Besmer, P. (1990a). Candidate ligand for the c-*kit* transmembrane kinase receptor: KL, a fibroblast derived growth factor stimulates mast cells and erythroid progenitors. *EMBO J.* **9**, 3287-3294.

Nocka, K., Tan, J. C., Chiu, E., Chu, T. Y., Ray, P., Traktman, P. and Besmer, P. (1990b). Molecular bases of dominant negative and loss of function mutations at the murine c-*kit*/white spotting locus: W^{37}, W^{v}, W^{41}, *W*. *EMBO J.* **9**, 1805-1813.

Nocka, K., Huang, E., Beier, D. R., Chu, T. Y., Buck, J., Lahm, H. W., Wellner, D. Leder, P. and Besmer, P. (1990c). The hematopoietic growth factor KL is encoded by the SL locus and is the ligand of the c-*kit* receptor, the gene product of the *W* locus. *Cell* **63**, 225-333.

Qiu, F., Ray, P., Brown, K., Parker, P. E., Jhanwar, S., Ruddle, F. H. and Besmer, P. (1988). Primary structure of c-*kit*: Relationship with the CSF-1/PDGF receptor kinase family - oncogenic activation of v-*kit* involves deletion of extracellular domain and C terminus. *EMBO J.* **7**, 1003-1011.

Rawles, M. E. (1947). Origin of pigment cells from the neural crest in the mouse embryo. *Physiol. Zool.* **20**, 248-265.

Reith, A. D., Rottapel, R., Giddens, E., Brady, C., Forrester, L. and Bernstein, A. (1990). W mutant mice with mild or severe developmental defects contain distinct point mutations in the kinase domain of the c-*kit* receptor. *Genes Dev.* **4**, 390-400.

Russell, E. S. (1979). Hereditary anemias of the mouse. *Adv. Genet.* **20**, 357-459.

Sambrook, J., Fritsch, E. F. and Maniatis, T. (1989). *Molecular Cloning, a Laboratory Manual* (ed 2). Cold Spring Harbor Laboratory: Cold Spring Harbor, NY.

Serbedzija, G. N., Fraser, S. E. and Bronner-Fraser, M. (1990). Pathways of trunk neural crest cell migration in the mouse embryo as revealed by vital dye labeling. *Development* **108**, 605-612.

Silvers, W. K. (1956). Pigment cells: Occurrence in hair follicles. *J. Morphol.* **99**, 41-55.

Silvers, W. K. (1979). *The Coat Colors of Mice.* New York: Springer-Verlag.

Smith, E. A., Seldin, M. F., Martinez, L., Watson, M. L., Choudhury, G. G., Lalley, P. A., Pierce, J., Aaronson, S., Barker, J., Naylor, S. L. and Sakaguchi, A. Y. (1991). Mouse platelet-derived growth factor receptor α gene is deleted in W^{19H} and *patch* mutations on chromosome 5. *Proc. Natl. Acad. Sci. USA* **88**, 4811-4815.

Stephenson, D. A., Glenister, P. H. and Hornby, J. (1985). Site of beige (bg) and leaden (ln) pigment gene expression determined by recombinant embryonic skin grafts and aggregation mouse chimeras employing sash (W^{sh}) homozygotes. *Genet. Res., Camb.* **46**, 193-205.

Stephenson, D. A., Mercola, M., Anderson, E., Wang, C., Stiles, C. D., Bowen-Pope, D. F. and Chapman, V. M. (1991). Platelet-derived growth factor receptor a-subunit gene (PDGFRA) is deleted in the mouse patch (Ph) mutation. *Proc. Natl. Acad. Sci. USA* **88**, 6-10.

Stevens, J. and Loutit, J. F. (1982). Mast cells in mutant mice (*W Ph mi*). *Proc. Roy. Soc. Lond. B.* **215**, 405-409.

Tan, J. C., Nocka, K., Ray, P., Traktman, P. and Besmer, P. (1990). The dominant W^{42} phenotype results from a missense mutation in the c-*kit* receptor kinase. *Science* **247**, 209-212.

Tono, T., Tsujimura, T., Koshimizu, U., Kasugai, T., Adachi, S., Isozaki, K., Nishikawa, S., Morimoto, M., Nishimune, Y., Nomura, S. and Kitamura, Y. (1992). c-*kit* gene was not transcribed in cultured mast cells of mast cell-dficient W^{sh}/W^{sh} mice that have a normal number erythrocytes and a normal c-*kit* coding region. *Blood* **80**, 1448-1453.

Williams, D. E., Eisenmann, J., Baird, A., Rauch, C., Van Ness, K., March, C. J., Park, L. S., Martin, U., Mochizuki, D. J., Boswell, H. S., Burgess, G. S., Cosman, D. and Lyman, S. D. (1990). Identification of a ligand for the c-kit proto-oncogene. *Cell* **63**, 167-174.

Yarden, Y., Kuang, W. -J., Yang-Feng, T., Coussens, L., Munemitsu, S., Dull, T. J., Chen, E., Schlessinger, J., Francke, U. and Ullrich, A. (1987). Human proto-oncogene c-*kit*: A new cell surface receptor tyrosine kinase for an unidentified ligand. *EMBO J.* **6**, 3341-3351.

Yung, Y. P. and Moore M. A. S. (1982). Long-term in vitro culture of murine mast cells III. Discrimination of mast cell growth factor and granulocyte-CSF. *J. Immunol.* **129**, 1256-1261.

Zelenetz, A. D., Chu, G., Galili, N., Bangs, C. D., Horning, S. J., Donlon, T. A., Cleary, M. L. and Levy, R. (1991). Enhanced detection of the t(14;18) translocation in malignant lymphioma using pulsed-field gel electrophoresis. *Blood* **78**, 1552-1560.

Zsebo, K. M., Wypych, J., McNiece, I. K., Lu, H. S., Smith, K. A., Karkare, S. B., Sachdev, R. K., Yuschenkoff, V. N., Birkett, N. C., Williams, R. L., Satyagal, V. N., Tung, W., Bosselman, R. A., Mendiaz, E. A. and Langley, K. E. (1990a). Identification, Purification, and biological characterization of hematopoietic stem cell factor from Buffalo rat liver conditioned medium. *Cell* **63**, 195-201.

Zsebo, K. M., Williams, D. A., Geissler, E. N., Broudy, V. C., Martin, F. H., Atkins, H. L., Hsu, R. Y., Birkett, N. C, Okino, K. H., Murdock, D. C., Jacobsen, F. W., Takeishi, T., Cattanach, B. M., Galli, S. J. and Suggs, S. V. (1990b). Stem cell factor is encoded at the Sl locus of the mouse and is the ligand for the c-*kit* tyrosine kinase receptor. *Cell* **63**, 213-224.

(Accepted 15 April 1993)